JOURNAL OF VIROLOGY, Aug. 1991, p. 3986–3994
0022-538X/91/083986-09$02.00/0

Vol. 65, No. 8

Monoclonal Antibody-Defined Epitope Map of Expressed Rubella Virus Protein Domains

JERRY S. WOLINSKY,[1]* MICHELINE McCARTHY,[1] OLIVE ALLEN-CANNADY,[1] WILLIAM T. MOORE,[2] RUI JIN,[1] SHI-NIAN CAO,[1] AMY LOVETT,[1] AND DENISE SIMMONS[1]

Department of Neurology[1] and Analytical Chemistry Center,[2] The University of Texas Health Science Center at Houston, P.O. Box 20708, Houston, Texas 77225

Received 12 December 1990/Accepted 17 April 1991

An expanded library of murine monoclonal antibodies (MAbs) was generated by infecting BALB/C mice with the Therien strain of rubella virus (RV) and selecting secreting hybrids by enzyme-linked immunosorbent assay (ELISA) using purified virion targets. A panel of plasmids containing specified RV cDNA fragments was also constructed by using a variety of strategies with pGE374- and pGE374-derived expression vectors. Hybrid RecA–RV–β-galactosidase (LacZ)- or RecA–RV-truncated LacZ-containing proteins collectively representing the entire open reading frame of the structural proteins of RV were overexpressed in *Escherichia coli*. Bacterial lysates were then probed by ELISA with selected MAbs and by immunoblot following separation by electrophoresis under denaturing conditions. With this approach, MAbs that appeared to react with linear determinants defined epitopes localized within the following domains: MAbs C-1, C-2, and C-8 bind epitopes within the predicted amino-terminal 21 amino acids of the capsid region C_9 to C_{29}; MAb C-9 binds to a domain bounded by C_{64} and C_{97}; MAbs E2-1 through E2-6 bind to the E2 glycoprotein backbone region from $E2_1$ to $E2_{115}$; MAbs E1-18 and E1-20 bind to the E1 glycoprotein region from $E1_{202}$ to $E1_{283}$. MAb E1-18 neutralizes RV infectivity; MAb E1-20 neutralizes infectivity and modestly inhibits hemagglutination. Analyses with selected synthetic peptides have confirmed several of the molecular domains deduced with the expressed proteins. These plasmid constructions and peptides have proven useful in beginning to unravel the molecular organization of several antigenic sites of this human pathogen.

Rubella virus (RV) is a togavirus and the sole representative of the *Rubivirus* subgroup. It is distinct from the alphaviruses in that it does not require an invertebrate vector for transmission of infection and has no known mammalian hosts other than humans (45). The identification, number, location, and functional importance of the structural proteins of RV have in large part been resolved. The virion contains three structural proteins designated E1, E2, and C (3, 28, 37, 39). The E1 glycoprotein bears the majority of the monoclonal antibody (MAb)-defined erythrocyte-binding and neutralization sites (14, 15, 17, 36, 40). The nucleotide sequence of the entire RV gene recently also has been resolved (7, 10–12, 26, 33, 34, 38).

RV infection can be associated with varied clinical outcomes, some of which may be immune mediated (46). To begin to explore in greater depth the naturally occurring host immune responses to RV, we have constructed a map of selected epitopes of the structural proteins of RV recognized by murine humoral responses during the course of an experimental infection. Specifically, MAbs were generated following RV infection of BALB/C mice. A subset of MAbs that recognized conformation-independent epitopes of RV was used to define selected epitope-containing domains of the genome when expressed as fusion proteins in a prokaryotic system. Several of these domains have been confirmed and further refined by the use of synthetic peptides.

MATERIALS AND METHODS

MAbs. The generation and characterization of several of the MAbs used in this study have previously been reported (39–41). To develop additional MAbs, 2- to 4-week-old male BALB/C mice were, as in the past, immunized by infection with one or more intraperitoneal injections of 0.5 ml of live Therien strain RV (~10^6 PFU). These mice received an additional intrasplenic injection of 0.1 ml of live RV 4 days prior to spleen harvest to obtain mononuclear cells for fusion with an NS-1 hybridoma partner (31). Following several fusions, the selection procedure was biased by using sodium dodecyl sulfate (SDS)- and dithiothreitol (DTT)-treated rubella virions as the target antigen in an otherwise standard enzyme linked immunosorbent assay (ELISA) (27). Hybridoma cell lines were established by cloning in soft agar (13); clones secreting MAbs of interest were expanded, and ascites fluid was produced by standard methods.

The specificity of each MAb was determined by immunoprecipitation of RV-infected Vero cell lysates. The MAb isotypes were defined by ELISA, using commercially available isotype-specific reagents (Bio-Rad, Richmond, Calif.). The capacity of each MAb to neutralize virus infectivity or inhibit hemagglutination was determined as previously detailed (40) except that ascites fluids were pretreated with heparin-manganese chloride when required (44).

Preparation of radiolabeled cell lysates. Confluent Vero cell monolayers grown in 25-cm^2 culture flasks in minimum essential medium containing 2% fetal bovine serum were infected at a multiplicity of infection of 1.0 with RV or mock infected to serve as controls. Five days into the infection, the medium was replaced with minimal essential medium deficient in the appropriate amino acid and the cells were incubated at 37°C for 60 min. The deficient medium was then replaced with 2 ml of deficient medium containing 200 μCi of L-[^{35}S]methionine (specific activity, 1,300 Ci/mmol; Amersham Corp., Arlington Heights, Ill.) per ml, 200 μCi of L-[^{35}S]cysteine (specific activity, 1,000 Ci/mmol; Amersham) per ml, 50 μCi of D-[6-^{3}H]glucosamine (specific activity, 40

* Corresponding author.

Ci/mmol; ICN Biomedicals, Inc., Costa Mesa, Calif.) per ml, or 50 μCi of D-[2-^{3}H]mannose (specific activity, 25 Ci/mmol; ICN) per ml, and the cells were incubated for 2 h at 37°C. Cell extracts were then prepared as previously detailed and stored at −80°C (40). Lysates were clarified by centrifugation in a Beckman Microfuge at 12,000 × *g* for 10 min just before use in the immunoprecipitation assay.

Immunoprecipitation and SDS-polyacrylamide electrophoresis (PAGE). Immunoprecipitation assays were performed as described previously (9). Briefly, 5 μl of crude ascites fluid or purified antibody was added to 20 μl of Sepharose-coupled protein A (Pharmacia, Pleasant Hill, Calif.) and 500 μl of lysate wash buffer (1% Triton X-100–0.5% sodium deoxycholate–0.1% SDS–0.5 M NaCl in 10 mM Tris, pH 7.4) in a 1.5-ml polypropylene tube and incubated at 4°C for 90 min with continuous tumbling. Unabsorbed antibody was removed by repetitively sedimenting and resuspending the immunoadsorbents in lysate wash buffer in a microfuge at 300 × *g*. An aliquot of radiolabeled cell lysate (usually ~10^7 dpm) was added to each assay tube in a total reaction volume of 500 μl and incubated for 90 min at 4°C with continuous tumbling. Unabsorbed molecules were removed by repetitive sedimenting and washing; the two final washes were with 10 mM Tris, pH 7.4. Bound radioactive molecules were then released by boiling for 5 min in 100 μl of SDS-sample buffer and analyzed by SDS-PAGE in 10% acrylamide resolving gels using a discontinuous buffer system followed by fluorography.

Enzyme digestion of immunoprecipitates. For these studies, washed immune complexes (polypeptide-MAb-protein A-Sepharose; see above) were resuspended in a minimal volume of 10 mM Tris to which was added 25 μl of a 200-μg/ml solution of either trypsin-tolylsulfonyl phenylalanyl chloromethyl ketone (TPCK) or endopeptidase Glu-C (Worthington Biochemical Corp., Freehold, N.J.). Digestion proceeded at 37°C for various times up to 24 h with constant tumbling; the standard digestion time was 60 min. The reaction was stopped by the addition of 25 μl of a 200-μg/ml solution of the trypsin inhibitor tolyllysine chloromethyl ketone, and the Sepharose complexes were extensively washed in immune lysate wash buffer followed by 10 mM Tris. The bound complexes were then disrupted in SDS-PAGE sample buffer for analysis of the antibody-protected domain in a 20% acrylamide resolving gel as described by others (4, 30).

Plaque reduction assay. A predetermined amount of RV containing 50 PFU was added to 10-fold dilutions of crude ascites fluid or purified MAb in Hanks balanced salt solution (HBSS) containing 0.1% bovine serum albumin and incubated for 1 h at room temperature. A 0.5-ml aliquot of each sample was inoculated into each of three monolayers of Vero cells grown in 35-mm plastic petri dishes that had been washed once with HBSS. The monolayers were then incubated at 37°C for 2 h. The inoculum was aspirated, the monolayers washed once with HBSS, and 2.5 ml of minimal essential medium containing 2.0% fetal bovine serum and 0.5% agarose (SeaKem HGT; FMC BioProducts, Rockland, Maine) was added to each plate. The agarose was hardened at room temperature, and the plates were incubated at 37°C for 5 to 6 days (40). The number of plaques was determined following application of the vital dye neutral red.

Immunoblotting. The electrophoretic transfer of proteins from SDS-PAGE to nitrocellulose paper (BA83; 0.2-μm pore size; Schleicher & Schuell, Inc., Keene, N.H.) was done according to minor modifications of the method of Towbin et al. (35), using a Trans-Blot apparatus (Bio-Rad). Transfer buffer consisted of 25 mM Tris, pH 8.3, with 192 mM glycine and 15 to 20% methanol. Transfer was effected at 50 V constant overnight. The nitrocellulose paper was rinsed briefly in TBST (10 mM Tris-HCl, pH 8.0, 150 mM NaCl, 0.05% Tween 20), followed by a 30-min blocking step in 1% nonfat dried milk in phosphate-buffered saline (PBS). The nitrocellulose paper was then incubated with appropriate dilutions of crude ascites fluid, a mouse anti-LacZ MAb (Promega, Madison, Wis.), or a polyvalent rabbit anti-RecA antiserum (22) in 1% milk-PBS for 90 min at 37°C with constant rocking. The membranes were then rinsed with TBST, and an alkaline phosphatase-conjugated anti-mouse or anti-rabbit reagent (Promega) was added. After further incubation and rinse steps, the membrane was removed and an insoluble color product was developed, using nitroblue tetrazolium and 5-bromo-4-chloro-3-indolyl phosphate as substrates. High- and low-range prestained molecular weight standards (Diversified Biotech, Newton, Mass., and Pharmacia LKB Biotech, Inc., Piscataway, N.J.) were included in the end lanes of the original gel for approximation of the molecular weights of immunolabeled proteins.

Expression vectors system and RV hybrid protein constructions. The open reading frame vector pGE374 was used for these studies (42, 43). This vector contains the *recA* promoter immediately upstream of the nucleotide sequence for the amino acids of RecA protein, followed out of open reading frame by the sequence of the β-galactosidase (*lacZ*) gene. Insertion and ligation of the appropriate RV cDNA genomic fragments at *Nco*I, *Sma*I, and *Bam*HI restriction sites conveniently located between these two sequences of pGE374 reestablishes the proper open reading frame to provide enzymatically based selection of transformed bacterial colonies of interest (22). The vector pGE372 contains the *recA* and *lacZ* genes fused in sequence with retained *Nco*I and *Bam*HI restriction sites. Depending on the insertion site used in pGE374, the expressed trihybrid protein should consist of 35 residues from RecA, a short stretch of up to 8 additional amino acids, the RV-expressed sequence, up to three junctional residues, and 1,007 amino acids from LacZ. Selected colonies were then grown in liquid phase and induced to overexpress trihybrid protein with mitomycin, and sonicated extracts of the bacteria were prepared and probed for immunoreactivity with the panel of MAbs by ELISA and immunoblot analysis.

The vectors and derived constructs were propagated in the host *Escherichia coli* MC1061. A modification of pGE374, pGE374DBI, was fabricated by excision of the segment between the *Nco*I and *Bam*HI sites and insertion of the sequence 5′-CATGGGAGGCCTGCCGGCG-3′. This vector retains the unique *Nco*I and *Bam*HI sites and provides alternative blunt-end *Stu*I and *Nae*I restriction sites for polymerase chain reaction (PCR)-amplified cDNA segment insertions.

Several RV cDNAs were provided by Teryl K. Frey as inserts in plasmid pUC8. These included pRUB1001, pRUB1006, pRUB1012, and pRUB1015 (11, 12) and a previously unreported construct, pRUBSORF, which contains the entire open reading frame of the polyprotein precursor of all three structural proteins of RV. These plasmids were propagated in *E. coli* DK$^-$ cells, harvested, and restricted with *Eco*RI and *Hin*dIII, and the excised segments were purified by agarose gel electrophoresis using standard molecular biologic techniques (1). The RV cDNA was then restricted with appropriate endonucleases or Bal31 (Boehringer Mannheim Corp., Indianapolis, Ind.) specifically chosen to engineer them into the pGE374 expression vector

TABLE 1. Oligonucleotide primers

Primer	RV bases	Primer sequence (5'-3')[a]
01	9101–9078	CTGAGAGCCTATGACAGGCGTGAC
02	8855–8878	GGACCTGGTTGAGTACATTATGAA
07	7443–7424	TAGGAGGTGCCGCCATATCA
10	8252–8274	CGAGGAGGCTTTCACCTACCTCT
16	6507–6535	*CC*ATGGCTTCTACTACCCCCATCACTATGGA
17	9674–9659	*GGATCC*AAGTAGTACAAGCAT
19	9730–9713	*TTCACAGC*GTGGCCTAGTGCGGGTTT
20	9280–9291	*CCATGG*ATGTGCGTGTGA
21	7672–7650	AAGTCCATGGGCTTGGTATGACA
22	8855–8878	*CCATG*GACCTGGTTGAGTACATTATGAA
26	6760–6779	*AACCATGG*AAGAAACTCGCTCCCAGACT

[a] 5' nucleotide additions to primers 16, 20, 22, and 26 to create *Nco*I sites, to 17 to create a *Bam*HI site, and to 19 to create a *Dra*III site are shown in italics. Nucleotide substitutions to destroy (primer 16) or create (primers 21) *Nco*I sites are shown in bold.

linearized with *Sma*I or *Nco*I. Such constructs were arbitrarily designated by the restriction endonucleases used (e.g., pRN; *Rsa*I, *Nae*I).

Specific regions of the pRUBSORF plasmid were selected as templates to amplify RV cDNA by the PCR method. These products were then used to engineer several of the expression vector constructs. Template plasmid cDNA was purified as minipreps from pRUBSORF-transformed bacteria, and 10 to 15 ng was used for each amplification. Oligonucleotide primers were synthesized for these purposes by George E. Mark, Merck Sharp & Dohme, West Point, Pa., using automated phosphoramidite methodology (2). Alternatively, cDNA was directly amplified from oligo(dT)-primed avian myeloblastosis virus reverse transcriptase (Invitrogen Corp., San Diego, Calif.) first-strand cDNA products of total RNA isolated from RV-infected Vero cells with guanidium thiocyanate (6, 18). Primers successfully used are listed in Table 1; 15 pM of each primer pair was present in the reaction mixture with 200 mM each deoxynucleoside triphosphate, 15 mM $MgCl_2$, 2 U of *Taq* polymerase (Perkin-Elmer Cetus Corp., Norwalk, Conn.), and standard buffer in a reaction volume of 100 μl. The templates were denatured for 2 min at 95°C, primers were annealed for 2 min at 55°C, and chains were extended for 2 min at 72°C over 20 to 40 cycles. Amplified segments were purified by agarose gel electrophoresis and used directly for ligation into blunt sites in pGE374 or pGE374DBI or restricted for directional insertion at the *Nco*I and *Bam*HI or *Dra*III sites of the vectors. Such constructs were arbitrarily designated by the oligonucleotide primers used (e.g., pARV16-07).

Precise boundaries of RV protein segments expressed as hybrid molecules by the plasmid constructs were determined by limited sequencing of the plasmid-RV cDNA insertion sites and the intervening RV segment. A set of oligonucleotides was commercially synthesized (Genetic Designs, Inc., Houston, Tex.) specific for the DNA sequences that flank the *Nco*I and *Bam*HI restriction site regions of pGE374 and those downstream of the unique *Dra*III site. The forward or positive-sense primer, 5'-AACAATTTGGTAAAGGC-3', corresponds to a region just downstream of the *recA* promoter. The reverse or negative-sense primer, 5'-GGTTTTCCCAGT CACGA-3', is downstream of the *Bam*HI site; 5'-ATGCCG TGGGTTTCAATATTGGCTTCATCCA-3' is downstream of the *Dra*III site. These directionally specific primers were then used to sequence through the insertion sites by the dideoxynucleotide chain termination method for double-stranded templates (47). DNA synthesis was performed with either the large fragment of T7 DNA polymerase (Sequenase; United States Biochemical Corp., Cleveland, Ohio) or *Taq* polymerase (GeneAmpKit; Perkin-Elmer Cetus Corp.) according to manufacturer's instructions and with 7-deaza-2'-dGTP to reduce sequencing artifacts which were otherwise common due to the unusually G+C-rich RV genome.

Peptide synthesis. Peptides were synthesized by solid-phase methods based on standard *tert*-butyloxycarbonyl (tBOC) amino acid addition protocols similar to those developed by others (24), using an automated peptide synthesizer (model 430A; Applied Biosystems Inc. [ABI], Foster City, Calif.) controlled by standard ABI system software version 1.40 for 0.5 mM scale synthesis. The starting material was a BOC–C-terminal amino acid–OCH_2–Pam–copoly(styrene–1% divinylbenzene) resin. All tBOC amino acids were obtained from Peninsula Laboratories, Inc. (Belmont, Calif.) except tBOC histidine (Bachem, Inc., Torrance, Calif.). The side-chain-protecting groups were benzyl (Ser and Thr), 2-bromobenzyloxycarbonyl (Tyr), 2-chlorobenzyloxycarbonyl (Lys), benzyloxycarbonyl (His), 4-methylbenzyl (Cys), formyl (Trp), benzyl ester (Asp and Glu), and tosyl (Arg). All of the peptide synthesis chemicals were from ABI except trifluoroacetic acid (Halocarbon Products Corp., Hackensack, N.J.), dichloromethane, and dimethylformamide (Burdick and Jackson Brand, Baxter Scientific Products, McGaw Park, Ill.). Peptides were deprotected and cleaved from resin by treatment with anhydrous hydrogen fluoride in the presence of either anisole alone or anisole with dimethyl sulfide and ethanedithiol when methionine was present. The cleaved peptide and resin were then washed with peroxide-free ethyl ether, and the peptide was extracted from the resin with 15% acetic acid. If methionine was present, 2% β-mercaptoethanol was included. After an additional ethyl ether extraction, the peptides were lyophilized. Preparative hydrogen fluoride cleavages were performed commercially by Immuno-Dynamics, Inc. (La Jolla, Calif.).

To eliminate the possibility of false-negative solid-phase ELISA results due to incorrect assembly of synthetic peptides, stringent assessment of the structural status of the synthetic peptides was performed by fast atom bombardment-mass spectrometry (FABMS) (5) on the final hydrogen fluoride-derived product. For some peptides, structural assessment was performed stepwise by FABMS on analyte peptide released by micro-trifluoromethanesulfonic acid cleavage from selected peptide-resin aliquots automatically removed after each coupling cycle (25). In the case of one synthetic peptide (SP10), the full-length peptide did not give an adequate FABMS signal. However, stepwise FABMS assessment indicated that 60% of the peptide comprising the C-terminal portion of the molecule was correct. Structural validation of the N-terminal portion was provided by pulsed-liquid/gas-phase micro-Edman primary structure determination using an ABI model 477A automated protein sequencer.

RESULTS

Monoclonal antibody library. The strategy used to generate our library of MAbs was based on the assumption that RV infection of BALB/C mice would evoke an immune response which might approximate the human response to uncomplicated rubella. Following inoculation with RV, BALB/C mice undergo subclinical infection. Thus, the spectrum of MAbs derived from BALB/C mice should be repre-

TABLE 2. MAb characteristics

MAb[a]	Immunoglobulin G isotype[b]	Neutralization[c]	HAI[d]	Western[e]	Domain[f]
E1-3	2A	0	40	0	FP
E1-5	2B	0	640	0	FP
E1-7	2B	0	0	0	FP
E1-8	2A	0	5,120	0	FP
E1-10	2A	0	160	0	E1-10
E1-11	2A	0	>10,000	0	E1-10
E1-12	2A	0	>10,000	0	E1-12
E1-13	1	0	>10,000	0	FP
E1-14	2A	0	80	0	FP
E1-15	2B	+	>10,000	0	E1-17
E1-16	2A	+	5,120	0	NT
E1-17	2A	+	>10,000	0	E1-17
E1-18	1	+	0	+	FP
E1-19	2A	0	>10,000	0	FP
E1-19_2	2A	+	0	0	E1-19_2
E1-20	2A	+	40	+	E1-20
E1-21	1	+	>10,000	0	FP
E1-22	1	+	>10,000	+	FP
E1-23	2A	+	>10,000	0	E1-17
E1-24	2A	+	>10,000	0	E1-17
E1-25	1	0	0	0	NT
E1-26	2A	0	320	0	NT
E1-27	1	0	1,280	0	NT
E1-28	2B	0	>10,000	0	NT
E1-29	2B	0	>10,000	0	NT
E1-30	1	0	0	0	NT
E1-31	2A	0	>10,000	0	NT
E2-1	2A	0	0	+	E2-1
E2-2	2A	0	0	+	E2-1
E2-3	2A	0	0	+	E2-3
E2-4	2A	0	0	+	E2-1
E2-5	2A	0	0	+	E2-5
E2-6	2A	0	0	+	E2-3
C-1	2A	0	0	+	C-1
C-2	2A	0	0	+	C-1
C-3	2A	0	0	+	C-3
C-4	2B	0	0	0	C-4
C-5	1	0	0	+	C-3
C-6	2A	NT	0	0	C-4
C-7	2A	NT	0	0	C-3
C-8	3	NT	0	+	C-1
C-9	2B	NT	0	+	C-9

[a] Designated by immunoprecipitation as (E1,E2,C)-(antibody no.).
[b] Determined by ELISA with affinity-purified specific antibodies.
[c] Determined as negative (0) or positive (+) according to the ability of crude ascites fluid to inhibit >50% of plaques when used at dilutions $\geq 10^{-2}$ in the plaque reduction assay.
[d] HAI, reciprocal hemagglutination inhibition titer per milliliter of ascites fluid.
[e] Reactivity in Western blot procedure as reactive (+) or nonreactive (0).
[f] Prototype MAb-protected radiolabeled digestion fragment pattern. FP, MAb failed to consistently protect any radiolabeled fragment from trypsin digestion; NT, not tested.

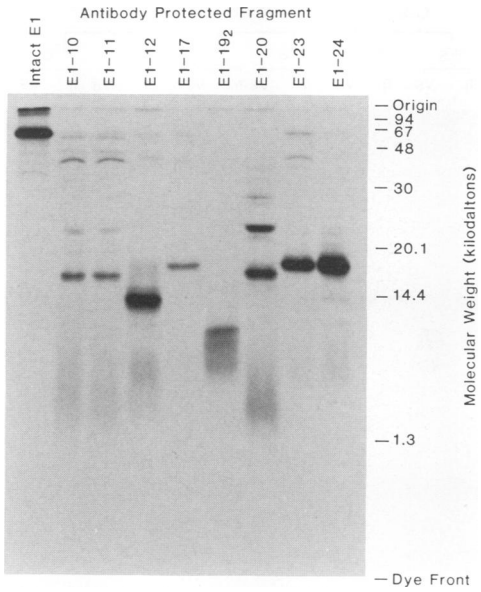

FIG. 1. MAb E1-protected digestion fragments. Lysates were made from RV-infected Vero cell monolayers radiolabeled with [^{35}S]methionine. Immunoprecipitates were then prepared by using various E1 series MAbs preadsorbed to protein A-Sepharose beads. Lane 1 shows a typical immunoprecipitate processed in the absence of trypsin. The immune complexes were then digested with trypsin-TPCK for 1 h at 37°C, washed, separated by SDS-PAGE using a 20% polyacrylamide resolving gel, and analyzed by fluorography as detailed in Materials and Methods. Samples processed in this manner are shown in the remaining lanes. Note the similarity of the radiolabeled protected fragment patterns between E1-10 and E1-11 and between E1-17, E1-23, and E1-24 and the unique patterns of E1-12, E1-19_2, and E1-20. A number of MAbs failed to consistently protect any radiolabeled fragment from digestion in this and similar experiments (data not shown).

sentative of the repertoire of humoral response which evolves in an intact immune system challenged by a virus fully capable of replication but, as is often the case in humans, unable to evoke clinical or histopathologic disease. Therefore, mice were infected and reinfected with live RV, and antibody-secreting hybridomas were selected by using a target of intact purified virions. The library of MAbs which resulted is shown in Table 2. Most but not all of the hybridomas remain viable and continue to secrete MAbs of defined specificity.

All of the MAbs have been characterized by specificity of binding to RV structural polypeptides in immunoprecipitation studies, using as targets radiolabeled infected cell lysates (see above). Our previous system of designation (39–41) has been retained so that MAbs reported in the past can be readily identified. MAbs E1-19_2 through E1-31, E2-2 through E2-6, and C-6 through C-9 have not previously been reported. The newer members of our E1 series MAbs show a similar range of properties in functional assays with RV, with some showing neutralization activity, hemagglutination inhibition, both activities, or neither activity. None of the E2 or C series MAbs inhibit these viral functions (Table 2).

Several of the E1 MAbs and all of the E2 and C MAbs have been further distinguished by their ability to protect radiolabeled infected cell lysate targets from digestion by site-specific endoproteases as described above. Figure 1 shows the results of such an experiment using selected E1 series MAbs, [^{35}S]methionine-labeled targets, and digestion with trypsin. Several distinct patterns of MAb-protected digestion fragments could readily be appreciated. Similar experiments using [^{3}H]glucosamine identified a carbohydrate component for the domains protected by E1-12-, E1-17-, and E1-20-type MAbs (data not shown). Figure 2 is an example of MAb-protected digestion studies done with the C series MAbs, using both [^{35}S]methionine- and [^{35}S]cysteine-labeled targets and either trypsin or endopeptidase Glu-C. Again, several unique MAb-protected digestion patterns emerged. The results of these and other studies not shown are summarized in Table 2.

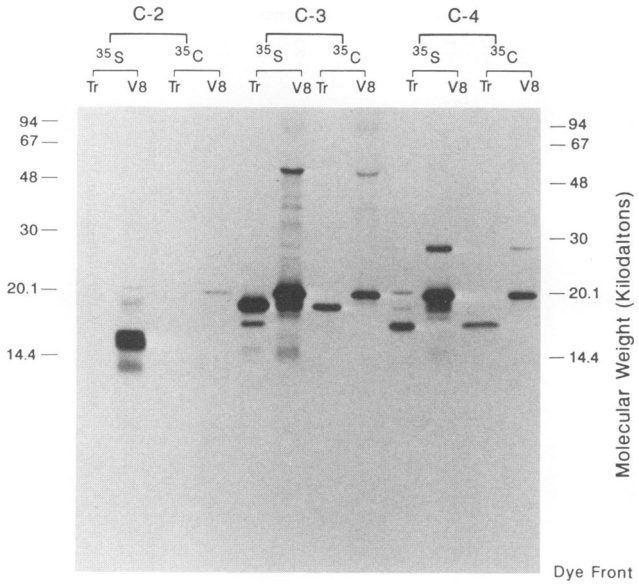

FIG. 2. MAb C-protected digestion fragments. Lysates were made from RV-infected Vero cell monolayers radiolabeled with either [^{35}S]methionine (^{35}S) or [^{35}S]cysteine (^{35}C). Immunoprecipitates were then prepared by using various C series MAbs preadsorbed to protein A-Sepharose beads. The immune complexes were then digested with either trypsin-TPCK (Tr) or endoproteinase Glu-C (V8) for 1 hr at 37°C, washed, separated by SDS-PAGE using a 20% polyacrylamide resolving gel, and analyzed by fluorography as detailed in Materials and Methods. The pattern of radiolabeled fragment protection shown for C-2 is representative of that seen with either C-1, C-2, or C-8; the C-3 pattern is characteristic of that seen with C-3, C-5, or C-7; and the C-4 pattern is typical of that seen for both C-4 and C-6. C-9 fails to protect any radiolabeled fragments in this type of analysis (data not shown).

Of the 27 distinct hybridoma products with specificity of binding for E1, only 3 (E1-18, E1-20, and E1-22) retain their capacity to react with the E1 glycoprotein molecule following disruption of RV by SDS-DTT and boiling, separation of the polypeptides by PAGE, and transfer to nitrocellulose membranes (data not shown). Thus, this subset of MAbs presumably defines epitopes of the contiguous or linear type. While most of the E1 MAbs tested fail to bind to their epitopes under these conditions and presumably define conformation-dependent or assembled epitopes, the two classes of E1 MAbs have similar types of activities in functional assays with intact virions (Table 2). In contrast, all of the E2-specific MAbs and the majority of the C-reactive MAbs appear to define contiguous epitopes. It was therefore this subset of MAbs reactive with linear epitopes that was selected for mapping those epitopes of the structural polypeptides of RV which would most likely yield to their deduction in molecular terms.

Plasmid constructs. A number of constructs of portions of the RV genome into pGE374 and related vectors have been made and analyzed. The panel of constructs used is shown in detail in Table 3. These include pRN (C_{-13} to C_{30}), pBstUI (C_{64} to C_{97}), pARV26-07 (C_{84} to $E2_{13}$), pB5 (C_{117} to $E2_{115}$), pN5 (C_9 to $E2_{216}$), pCV ($E2_{132}$ to $E1_{97}$), pARV10-01 ($E1_1$ to $E1_{283}$), p9 ($E1_{162}$ to $E1_{332}$), pARV02-01 ($E1_{202}$ to $E1_{283}$), pARV22-19 ($E1_{202}$ to $E1_{481}$), and pARV20-17 ($E1_{344}$ to $E1_{474}$); the amino acid residues are numbered according to the numbering of Dominguez et al. (10). Together, the hybrid

TABLE 3. Plasmid constructions

Plasmid	Protein	Method
pRN	$RecA_{1-35}$-GIGDLGSP-C_{-13}-C_{30}-DP-$LacZ_{9-1015}$	pGE374 + *Sma*I-*Rsa*I + *Nae*I
pBstUI	$RecA_{1-35}$-GIGDLGSP-C_{64}-C_{97}-GDP-$LacZ_{9-1015}$	pGE374 + *Sma*I-*Bst*UI
pARV26-07	$RecA_{1-35}$-E-C_{84}-$E2_{13}$-CRRIPSFYNVVTGKTLALPNLIALQHIPLSPAGVIAKRPAPIALPNSCAA	pGE374DBI + *Nco*I + *Stu*I (PCR)
pB5	$RecA_{1-35}$-GIGDLGSP-C_{117}-$E2_{115}$-GDP-$LacZ_{9-1015}$	pGE374 + *Sma*I-Bal 31
pN5	$RecA_{1-34}$-C_9-$E2_{216}$-IGDLGSPGIPSFYNVVTGKTLALPNLIALQHIPLSPAGVIAKRPAPIALPNSCAA	pGE374 + *Nco*I-*Nco*I
pCV	$RecA_{1-35}$-GIGNDGSP-$E2_{132}$-$E1_{97}$-DP-$LacZ_{9-1015}$	pGE374 + *Sma*I-*Alu*I
pARV10-01	$RecA_{1-35}$-GG-$E1_1$-$E1_{283}$-PAGGSRRFTTS	pGE374DBI + *Stu*I (PCR)
p9	$RecA_{1-35}$-GIGDLGSP-$E1_{162}$-$E1_{332}$-DP-$LacZ_{9-1015}$	pGE374 + *Sma*I-Bal 31
pARV02-01	$RecA_{1-35}$-GIGDLGSP-$E1_{202}$-$E1_{283}$-GDP-$LacZ_{9-1015}$	pGE374 + *Sma*I (PCR)
pARV22-19	$RecA_{1-35}$-$E1_{202}$-$E1_{481}$	pGE372 + *Nco*I + *Dra*III (PCR)
pARV20-17	$RecA_{1-35}$-D-$E1_{344}$-$E1_{474}$-DP-$LacZ_{9-1015}$	pGE372 + *Nco*I + *Bam*HI (PCR)

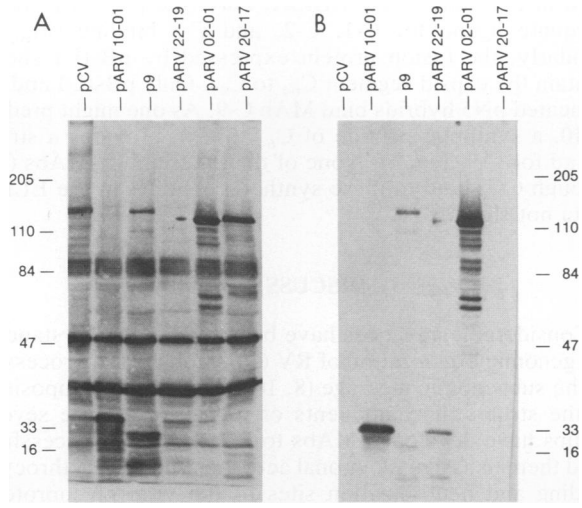

FIG. 3. Western blot analysis of E1 region-expressed hybrid proteins for anti-RecA and E1-18 binding. Transformed, induced bacteria were harvested, pelleted, and processed for analysis by SDS-PAGE under reduced conditions. Separated proteins were then transferred to nitrocellulose. Since RecA is a constituent protein of the *E. coli lon* strain used, a number of immunoreactive bands are apparent in each of the lanes when a polyvalent rabbit anti-RecA antibody was used as a probe (A). Nontheless, unique fusion protein is evident in each of the lanes whose molecular weight corresponds to that predicted for each construct. In contrast, only selected fusion proteins were detected when the other half of this membrane to which identical samples had been transferred was probed with the neutralizing MAb E1-18 (B).

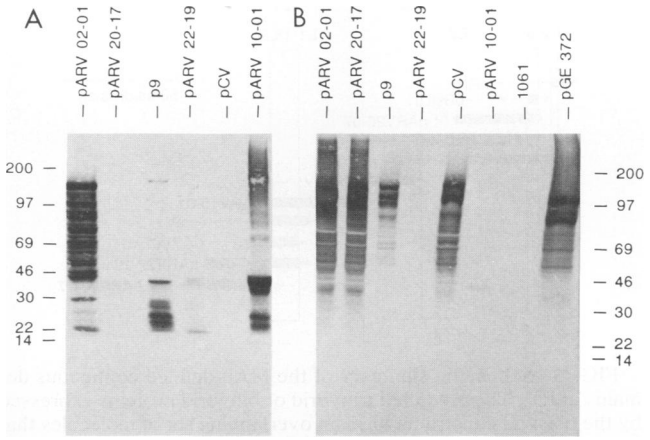

FIG. 4. Western blot analysis of E1 region-expressed hybrid proteins for E1-20 and anti-LacZ binding. Transformed, induced MC1061 bacteria were harvested, pelleted, and processed for analysis by SDS-PAGE under reduced conditions. Separated proteins were then transferred to nitrocellulose. The MAb E1-20-probed membrane (A) shows a plasmid-specific pattern. A similar preparation was probed with a commercial murine anti-LacZ MAb (B). Proteins from untransformed *E. coli* (lane 1061) were unreactive. The RecA-LacZ bihybrid was seen at ~117 kDa in in-frame vector-only-transformed bacterial proteins (lane pGE372). Proteins from specific RV vector construct-transformed bacteria had variable molecular weights consistent with their predicted amino acid content. Sizes are indicated in kilodaltons.

proteins expressed by these plasmid constructs provide overlapping target molecules which are representative of the protein backbones of the structural polypeptides of the rubella virion. Proteins harvested from bacteria expressing these plasmids were probed with selected MAbs in both ELISA and Western immunoblot analyses.

Figures 3 and 4 are representative of the results obtained with immunoblots of SDS-DTT-treated and PAGE-separated sonic extracts of mitomycin-induced cultures of *E. coli* MC1061 or a protease-deficient *lon* mutant transformed with those plasmids predicted to express hybrid proteins which span the E1 polypeptide region. The gel shown in Fig. 3A was probed with a rabbit monospecific anti-RecA serum. As RecA is a constituently expressed protein of both MC1061 and the *lon* mutant, it is overexpressed in the presence or absence of mitomycin. Thus, several bands, including prominent species of about 44 and 33 kDa, are common to each of the transformed bacterial preparations. However, a unique band that reflects the hybrid molecule encoded by the plasmid is evident for each of the transformed bacterial preparations. The gel shown in Fig. 3B was probed with MAb E1-18; only preparations from pARV10-01, p9, pARV02-01, and pARV22-19 express immunoreactive proteins. The relative amount of hybrid protein expressed was a reproducible feature of each plasmid. This variability among plasmids was at least in part due to different degradation rates of the expressed hybrid in the MC1061 host. In general, we have obtained different breakdown patterns and better total yields of the intact hybrid proteins when selected plasmids are propagated and expressed in *lon* mutants (data not shown).

The gel shown in Fig. 4B was probed with a murine anti-LacZ MAb. Unlike RecA, LacZ is not a constituent protein of MC1061. Therefore, it is not expressed in the absence of transformation with a plasmid containing the *lacZ* gene in proper reading frame under the control of the *recA* promoter. Following induction with mitomycin, several bands, including a prominent predicted high-molecular-weight species and a ladder of related lower-molecular-weight spontaneous cleavage products, are found in bacterial preparations transformed with such constructs; otherwise the preparations remain unstained. Figure 4A shows the results when E1-20 was used as the probe. An unique band pattern is evident for several but not all of the transformed bacterial preparations. The unique band reflects the presence of a hybrid molecule expressing the domain that contains the epitope defined by this MAb. Taken together, these results suggest that the E1-18 and E1-20 epitope sequences are contained within the domain of E1 defined by $E1_{202}$ to $E1_{283}$. The results of these and similar studies with the other MAbs that were presumed to define linear epitopes (data not shown) are schematically summarized in Fig. 5.

Synthetic peptides. The pRN-expressed trihybrid should contain a 42-amino-acid segment of RV, including 13 residues proximal to the predicted 5′-NH_2 terminus of C followed by the theoretical first N-terminal 30 amino acids of C. When proteins harvested from bacteria expressing this plasmid were probed with selected MAbs in both ELISA and Western blot analyses, the results demonstrated that the domain defined by MAbs C-1, C-2, and C-8 was expressed as summarized in Fig. 5. C-1, C-2, and C-8 have independently been determined to define several very closely spaced epitopes if not an identical epitope (Table 2; Fig. 3 and 5). The hybrid protein expressed with pN5 also serves as an excellent binding substrate for C-1, C-2, and C-8, even

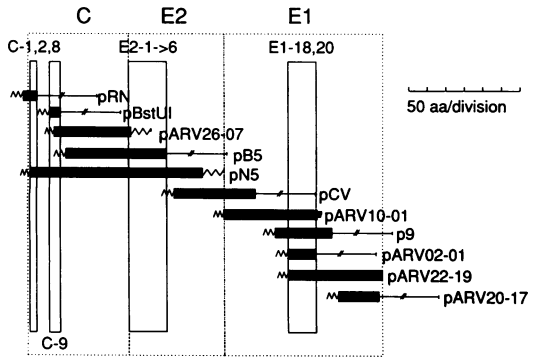

FIG. 5. Schematic summary of the MAb-defined contiguous domains of RV. The predicted trihybrid or bihybrid proteins expressed by the plasmid constructs form an overlapping set of molecules that are representative of the entire C, E2, and E1 structural backbones. The front squiggle is proportional to the size of the RecA segment, the solid block reflects the RV segment, and a trailing broken bar represents a complete and enzymatically functional LacZ. A trailing squiggle is proportional to a nonsense peptide tail. Absence of a tail for the pARV22-19 bihybrid reflects the presence of RV stop codons. MAbs C-1, C-2, and C-8 bind to a consensus amino-terminal region of 21 residues (C_9 to C_{29}), C-9 binds to a 34-residue block (C_{64} to C_{97}), the entire panel of E2 MAbs maps to a 116-residue domain at the amino terminus of the E2 backbone ($E2_1$ to $E2_{115}$), and a single domain of 82 amino acids ($E1_{202}$ to $E1_{283}$) is defined in the E1 region by E1-18 and E1-20. MAb C-5 appears to bind to a highly protease sensitive epitope in the carboxyl-terminal two-thirds of the capsid region (unpublished observations). Delineation of this site requires further optimization of the plasmid-host expression system.

though it was expressed as a truncated molecule of only about one-third of its predicted molecular mass. None of the other plasmids expressing fusion proteins of the capsid polypeptide bind these MAbs. This finding suggested a model for the C-1–C-2–C-8 domain which would encompass C_9 through C_{30}.

To further support the deduction, data were developed by using selected synthetic peptides. We fabricated several peptides that contain amino acid residues C_1 to C_{18} (SP1), C_{14} to C_{29} (SP2), C_9 to C_{29} (SP8), and C_9 to C_{22} (SP14). When used in our solid-phase ELISA, only SP8 proved to be an adequate ligand for C-1, C-2, and C-8 binding (Fig. 6). Similarly, the fusion protein expressed by pBstUI should contain the capsid segment C_{64} to C_{97}. Only pBstUI and the truncated pN5 hybrids bind MAb C-9. As one might predict, SP10, a synthetic peptide of C_{64} to C_{97}, provides a strong ligand for C-9 (Fig. 6). None of the other anti-C MAbs (C-3 through C-7) bind to these synthetic peptides in the ELISA (data not shown).

DISCUSSION

Considerable advances have been made in understanding the genomic organization of RV (10), steps in the processing of the subgenomic message (8, 16, 32), and the composition of the structural components of the virion. While several groups have developed MAbs to RV and have successfully used them to assign functional activities such as erythrocyte-binding and neutralization sites to the viral glycoproteins (14, 15, 17, 36, 40), few attempts have previously been made to reduce the MAb-defined epitopes of RV to molecular terms (34). However, such information is crucial for the development of reagents with which to probe in detail immune responses that arise following natural and vaccine-induced RV infections of humans or to contrast the normal pattern with aberrant immune responses which might occur in some individuals to give rise to some of the immediate or delayed complications of rubella (45). Our approach to this problem was to generate a library of murine MAbs in such a manner that they might reflect the repertoire of responses following natural infection in humans and evaluate a subset of these MAbs for their capacity to bind to expressed and synthetic peptides representing segments of the structural polypeptides of RV.

MAbs bind to their respective viral antigens through a complementarity of shapes of the binding pocket of the antibody and the surface topography of the corresponding epitope of the viral protein (21). The epitope can be formed from elements of nearly contiguous stretches of amino acids or from structure brought together by rather complex folding of the protein. Epitopes that superficially appear to be formed from contiguous sequences of amino acids are re-

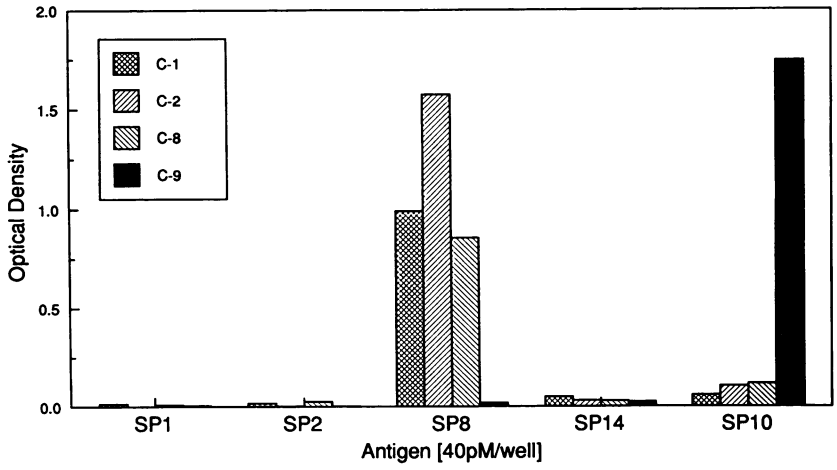

FIG. 6. Immunoreactivity profiles of MAbs with capsid region synthetic peptides. Synthetic peptides were bound to individual wells of 96-well microtiter plates at a concentration of 40 pmol per well, and various MAb-containing ascites fluids diluted 10^{-4} were added. All reactions were carried out in quadruplicate, using otherwise standard ELISA conditions.

ferred to as linear; those that arise from distant segments of a protein or are assembled from elements of independent protein subunits are termed noncontiguous. The latter are difficult to deduce in molecular terms or to synthesize artificially. In characterizing our library of MAbs, we initially sought to define those MAbs whose binding domains were unique by using several approaches, none of which proved entirely satisfactory for the purpose of deducing the binding domains in molecular terms (39–41). The use of reciprocal competitive inhibition studies to operationally define viral epitopes is commonplace but provides surprisingly little useful information on the molecular nature of the binding site involved in the absence of a broad-based panel of antibody-derived escape mutants or comparative data on binding patterns for a wide range of virus variants. Even then, in the absence of sequence or crystallographic data, this information is of limited utility. MAb-protected digestion studies are an additional means to subgroup MAbs of similar types, but in the absence of precise molecular mass determinations of the protected domains and sequence data, they also provide poor insight into the molecular organization of the epitopes involved.

Restricting our approach to define binding domains for those MAbs which appeared to react with epitopes that resist denaturation seems to have been more successful. Such MAbs form the majority of our library which are reactive with the C and E2 polypeptides but a minority of those specific for the E1 glycoprotein. Six of the nine anti-C MAbs bind to epitopes that resist denaturation. Four of these have been successfully mapped to domains of 32 or fewer amino acids. MAbs C-1, C-2, and C-8, which appeared to have similar targets as shown in antibody-protected digestion studies, were reactive with a similar group of expressed trihybrid proteins. The binding of these MAbs to the synthetic peptides has confirmed that a region spanning at most 20 capsid protein residues must contain the epitope(s) defined by these MAbs. Further, immunization of mice with one of these synthetic peptides (SP8) induces a vigorous humoral immune response reactive with SP8 and also cross-reactive with RV in the ELISA assay (unpublished observations). Thus, the MAbs of the C-1–C-2–C-8 domain and their respective epitopes must be restricted within the sequence C_9 to C_{29}. It also follows that SP8 not only provides an adequate conformation for MAb binding but appears sufficient to induce an antibody response of quality similar to that produced by the MAbs generated in the course of a subclinical RV infection.

The domain containing the MAb C-9-defined epitope similarly has been replicated as a synthetic peptide (SP10). This is an epitope of possible singular interest. MAb C-9 has been shown to cross-react with a 52-kDa molecule of rat pancreatic islet tumor cells (20). The 52-kDa molecule is also known to bind antibody from the sera of nonobese diabetic mice that have spontaneously developed anti-islet cell antibodies; a proportion of human sera from patients with type I diabetes mellitus are also reactive with this molecule (19). Thus, one could envision that this similarity of shape if not of primary amino acid sequence of the MAb C-9-defined RV epitope and a site on the 52-kDa protein might be important in understanding some of the late consequences of congenital rubella through some form of molecular mimicry (29).

The domains defined by anti-E2 and anti-E1 series MAbs remain relatively large. While it should be possible to reduce the domain containing epitopes of all of the E2 MAbs to synthetic peptides, only the antibody-protected digestion studies thus far suggest that these MAbs will define more than one epitope of this large region. The domain containing the epitope(s) defined by MAbs E1-18 and E1-20 is also relatively large but is more readily amenable to analysis using a reasonable number of overlapping synthetic peptides created on the basis of the primary sequence of this domain. The possibility that these epitopes reflect portions of the E1 glycoprotein critical for the binding of virus to the surface of erythrocytes or, more importantly, the host cell membrane or are intimately involved in critical virus-host cell interactions characteristic of early stages of infection is suggested by the functional activities of these MAbs (Table 2). Others have also identified this region of E1 as a potentially important site for the erythrocyte agglutination and infectivity of the intact virus by using different approaches and either MAbs (34) or pooled human RV-seropositive serum (23).

In conclusion, our approach to mapping epitope-containing domains of RV of potential biologic significance by using a subset of MAbs generated during the course of a subclinical virus infection appears to have been successful in defining several domains that have been reduced to the level of synthetic peptides and other domains that will likely yield to a similar analysis, which is in progress. It remains to be seen whether those synthetic peptides developed through this work which represent native RV epitopes can be used to probe in a qualitative and quantitative fashion human lymphocytes in vitro or to evaluate human immune sera for specific functional qualities.

ACKNOWLEDGMENTS

We are indebted to Teryl Frey, Georgia State University, for providing the plasmids containing RV cDNA inserts and for sharing genomic sequence information prior to publication. George Mark, Merck Sharp & Dohme, was most generous in synthesizing the RV-specific oligonucleotides, and Julian Leibowitz, University of Texas Medical School, provided the polyvalent anti-RecA serum along with considerable encouragement. In addition to providing the pGE372 and pGE374 vectors, George Weinstock, University of Texas Medical School, was an invaluable resource in helping us adapt these plasmids for our purposes.

This study was supported in large part by grant AI26943 from the National Institutes of Health.

REFERENCES

1. **Ausubel, F. M., R. Brent, R. E. Kingston, D. D. Moore, J. G. Seidman, J. A. Smith, and K. Struhl.** 1989. Current protocols in molecular biology. John Wiley & Sons, New York.
2. **Beaucage, S. L., and M. H. Caruthers.** 1981. Deoxynucleoside phosphoramidites—a new class of key intermediates for deoxypolynucleotide synthesis. Tetrahedron Lett. **22**:1859–1862.
3. **Bowden, D. S., and E. G. Westaway.** 1984. Rubella virus: structural and non-structural proteins. J. Gen. Virol. **65**:933–943.
4. **Bricker, B. J., R. M. Snyder, J. W. Fox, W. A. Volk, and R. R. Wagner.** 1987. Monoclonal antibodies to the glycoprotein of vesicular stomatitis virus (New Jersey serotype): a method for preliminary mapping of epitopes. Virology **161**:533–540.
5. **Caprioli, R. C., and W. T. Moore.** 1990. Continuous-flow fast atom bombardment mass spectrometry. Methods Enzymol. **193**:214–237.
6. **Chomczynski, P., and N. Sacchi.** 1987. Single-step method of RNA isolation by acid guanidium thiocyanate-phenol-chloroform extraction. Anal. Biochem. **162**:156–159.
7. **Clarke, D. M., T. W. Loo, I. Hui, P. Chong, and S. Gillam.** 1987. Nucleotide sequence and in vitro expression of rubella virus 24S subgenomic messenger RNA encoding the structural proteins E1, E2 and C. Nucleic Acids Res. **15**:3041–3057.
8. **Clarke, D. M., T. W. Loo, H. McDonald, and S. Gillam.** 1988. Expression of rubella virus cDNA coding for the structural proteins. Gene **65**:23–30.

9. **DeMazancourt, A., M. N. Waxham, J. C. Nicholas, and J. S. Wolinsky.** 1986. Antibody response to the rubella virus structural proteins in infants with the congenital rubella syndrome. J. Med. Virol. **19**:111–122.
10. **Dominguez, G., C.-Y. Wang, and T. K. Frey.** 1990. Sequence of the genome RNA of rubella virus: evidence for genetic rearrangement during togavirus evolution. Virology **177**:225–238.
11. **Frey, T. K., and L. D. Marr.** 1988. Sequence of the region coding for virion proteins C and E2 and the carboxy terminus of the nonstructural proteins of rubella virus: comparison with alphaviruses. Gene **62**:85–99.
12. **Frey, T. K., L. D. Marr, M. L. Hemphill, and G. Dominguez.** 1986. Molecular cloning and sequencing of the region of the rubella virus genome coding for glycoprotein E1. Virology **154**:228–232.
13. **Galfre, G., and C. Milstein.** 1981. Preparation of monoclonal antibodies: strategies and procedures. Methods Enzym **73**:3–46.
14. **Gerna, G., M. G. Revello, M. Dovis, E. Petruzzelli, G. Achilli, E. Percivalle, and M. Torsellini.** 1987. Synergistic neutralization of rubella virus by monoclonal antibodies to viral haemagglutinin. J. Gen. Virol. **68**:2007–2021.
15. **Green, K. Y., and P. H. Dorsett.** 1986. Rubella virus antigens: localization of epitopes involved. J. Virol. **57**:893–898.
16. **Hobman, T. C., and S. Gillam.** 1989. In vitro and in vivo expression of rubella virus glycoprotein-E2: the signal peptide is contained in the C-terminal region of capsid protein. Virology **173**:241–250.
17. **Ho-Terry, L., and A. Cohen.** 1985. Rubella virus hemagglutinin: association with a single virion glycoprotein. Arch. Virol. **84**:207–215.
18. **Innis, M. A., D. H. Gelfand, J. J. Sninsky, and T. J. White.** 1990. PCR protocols. A guide to methods and applications. Academic Press, Inc., San Diego, Calif.
19. **Karounos, D. G., and J. W. Thomas.** 1990. Recognition of common islet antigen by autoantibodies from NOD mice and humans with IDDM. Diabetes **39**:1085–1090.
20. **Karounos, D. G., J. S. Wolinsky, and J. W. Thomas.** Submitted for publication.
21. **Laver, W. G., G. M. Air, R. G. Webster, and S. J. Smith-Gill.** 1990. Epitopes on protein antigens: misconceptions and realities. Cell **61**:553–556.
22. **Leibowitz, J. L., S. Perlman, G. Weinstock, J. R. DeVries, C. Budzilowicz, J. M. Weissemann, and S. R. Weiss.** 1988. Detection of a murine coronavirus nonstructural protein encoded in a downstream open reading frame. Virology **164**:156–164.
23. **Lozzi, L., M. Rustici, M. Corti, M. G. Cusi, P. E. Valensin, L. Bracci, A. Santucci, P. Soldani, A. Spreafico, and P. Neri.** 1990. Structure of rubella E1 glycoprotein epitopes established by multiple peptide synthesis. Arch. Virol. **110**:271–276.
24. **Merrifield, R. B., L. D. Vizioli, and H. G. Boman.** 1982. Synthesis of the antibacterial peptide cecopin A(1-33). Biochemistry **21**:5020–5031.
25. **Moore, W. T., and R. C. Caprioli.** 1991. Monitoring peptide synthesis stepwise by mass spectrometry, p. 511–528. *In* J. Villafranca (ed.), Techniques in protein chemistry II. Academic Press, Inc., San Diego, Calif.
26. **Nakhasi, H. L., D. X. Zheng, L. Callahan, J. R. Dave, and T. Y. Liu.** 1989. Rubella virus—mechanism of attenuation in the vaccine strain (HPV77). Virus Res. **13**:231–243.
27. **Nath, A., B. Slagle, and J. S. Wolinsky.** 1989. Anti-idiotypic antibodies to rubella virus. Arch. Virol. **107**:159–167.
28. **Oker-Blom, C., N. Kalkkinen, L. Kääriäinen, and R. F. Pettersson.** 1983. Rubella virus contains one capsid protein and three envelope glycoproteins, E1, E2a and E2b. J. Virol. **46**:964–973.
29. **Oldstone, M. B. A.** 1989. Molecular mimicry as a mechanism for the cause and a probe uncovering etiologic agent(s) of autoimmune disease. Curr. Top. Microbiol. Immunol. **145**:127–135.
30. **Sheshberadaran, H., and L. G. Payne.** 1988. Protein antigen-monoclonal antibody contact sites investigated by limited proteolysis of monoclonal antibody-bound antigen: protein "footprinting". Proc. Natl. Acad. Sci. USA **85**:1–5.
31. **Sternick, J. L., and A. M. Sturmer.** 1984. A new high yielding immunization protocol for monoclonal antibody production against soluble antigens. Hybridoma **3**:74.
32. **Suomalainen, M., H. Garoff, and M. D. Baron.** 1990. The E2 signal sequence of rubella virus remains part of the capsid protein and confers membrane association in vitro. J. Virol. **64**:5500–5509.
33. **Takkinen, K., G. Vidgren, J. Ekstrand, U. Hellman, N. Kalkkinen, C. Wernstedt, and R. F. Pettersson.** 1988. Nucleotide sequence of the rubella virus capsid protein gene reveals an unusually high G/C content. J. Gen. Virol. **69**:603–612.
34. **Terry, G. M., L. Ho-Terry, P. Londesborough, and K. R. Rees.** 1988. Localization of the rubella E1 epitopes. Arch. Virol. **98**:189–197.
35. **Towbin, H., T. Staehelin, and J. Gordon.** 1979. Electrophoretic transfer of proteins from polyacrylamide gels to nitrocellulose sheets: procedure and some applications. Proc. Natl. Acad. Sci. USA **76**:4350–4354.
36. **Trudel, M., F. Nadon, C. Sequin, A. Amarouch, P. Payment, and S. Gillam.** 1985. E1 glycoprotein of rubella virus carries an epitope that binds a neutralizing antibody. J. Virol. Methods **12**:243–250.
37. **Vaheri, A., and T. Hovi.** 1972. Structural proteins and subunits of rubella virus. J. Virol. **9**:10–16.
38. **Vidgren, G., K. Takkinen, N. Kalkkinen, L. Kääriäinen, and R. F. Pettersson.** 1987. Nucleotide sequence of the genes coding for the membrane glycoproteins E1 and E2 of rubella virus. J. Gen. Virol. **68**:2347–2357.
39. **Waxham, M. N., and J. S. Wolinsky.** 1983. Immunochemical identification of rubella virus hemagglutinin. Virology **126**:194–203.
40. **Waxham, M. N., and J. S. Wolinsky.** 1985. Detailed immunologic analysis of the structural polypeptides of rubella virus using monoclonal antibodies. Virology **143**:153–165.
41. **Waxham, M. N., and J. S. Wolinsky.** 1985. A model of the structural organization of rubella virions. Rev. Infect. Dis. **7**:S133–S139.
42. **Weinstock, G. M.** 1984. Vectors for expressing open reading frame DNA in Escherichia coli using lacZ gene fusion, p. 31–48. *In* J. K. Setlow and A. Hollaender (ed.), Genetic engineering: principles and methods. Plenum Publishing Corp., New York.
43. **Weinstock, G. M., C. ap Rhys, M. L. Berman, B. Hampar, D. Jackson, T. J. Silhavy, J. Weisemann, and M. Zweig.** 1983. Open reading frame expression vectors: a general method for antigen production in Escherichia coli using protein fusions to beta galactosidase. Proc. Natl. Acad. Sci. USA **80**:4432–4436.
44. **Wittenburg, R. A., M. A. Roberts, L. B. Elliott, and L. M. Little.** 1985. Comparative evaluation of commercial rubella virus antibody kits. J. Clin. Microbiol. **21**:161–163.
45. **Wolinsky, J. S.** 1990. Rubella virus, p. 815–840. *In* B. N. Fields, D. M. Knipe, R. M. Chanock, J. L. Meinick, B. Roizman, and R: E. Shope (ed.), Virology. Raven Press, New York.
46. **Wolinsky, J. S.** 1990. Subacute sclerosing panencephalitis, progressive rubella panencephalitis and progressive multifocal leukoencephalopathy, p. 259–268. *In* B. H. Waksman (ed.), Immunologic mechanisms in neurologic and psychiatric disease. Raven Press, New York.
47. **Zhang, H., R. Scholl, J. Browse, and C. Somerville.** 1988. Double stranded DNA sequencing as a choice for DNA sequencing. Nucleic Acids Res. **16**:1220.